

A Novel Method for Rolling Bearing Fault Diagnosis Based on VMD and SGW

Toufik BENSANA*, Medkour MIHOUB**, Slimane MEKHILEF***, Mohamed FNIDES****

*The Higher School of Technological Education in Skikda, Azzaba Skikda, Algeria, E-mail: tbensana@gmail.com

**Laboratory of studies and research in industrial technology, Blida 1 University, Algeria

***Industrial Mechanics Laboratory (LMI), Badji Mokhtar University, BP 12, Annaba, Algeria

****The Higher School of Technological Education in Skikda, Azzaba Skikda, Algeria

crossref <http://dx.doi.org/10.5755/j02.mech.28531>

1. Introduction

Rolling element bearings are usually applied in rotating machinery and play an imperative role in current manufacturing industries. The malfunction of rolling element bearings results in the deterioration of machine performance; it is thus necessary to precisely identify faults in the bearings [1]. Vibration data is the most frequently employed for fault diagnosis of mechanical equipment. Since most of the bearing vibration data are non-linear and non-stationary, it is necessary to find a method to extract the effective features from the vibration signals which can be used in bearing fault diagnosis [2, 3].

Recently, adaptive signal analysis methods for nonstationary signals have attracted considerable attention, which can adaptively decompose a complex signal into multiple modes according to the intrinsic characteristics of a signal, and provide powerful tools for periodic impulses extraction and rolling bearings fault diagnosis. For example, the empirical mode decomposition (EMD) proposed by Huang has been widely studied and applied in the field of mechanical fault diagnosis [4, 5]. However, it has a major drawback, which is the mode mixing problem. Therefore, the ensemble EMD (EEMD) and other improved EMD methods are presented to alleviate the mode mixing problem in the EMD, and have been widely applied to fault diagnosis of rotating machinery [6, 7].

The local mean decomposition (LMD) proposed by Smith is an iterative approach to demodulating amplitude and frequency modulated signals, which can decompose any complicated signal into a set of product functions (PFs), and each PF is the product of an envelope signal and a frequency modulated signal [8, 9]. The comparisons of LMD and EMD have been done and the superiority of the LMD in fault diagnosis of rolling bearing has been verified [10]. In addition, as a non-recursive signal decomposition method, the variational mode decomposition (VMD) which combines Wiener filtering, Hilbert transform and frequency mixing techniques, and is a new completely non-recursive adaptive signal processing method [11]. The core idea of this method is to assume that each mode revolves around its own central frequency. The problem of solving modal bandwidth is transformed into a constrained optimization problem, and then each modal is calculated. Based on the unique advantages of VMD, this paper introduces it into fault diagnosis and proposes a fault diagnosis method based on VMD [12, 13]. Due to the influence of background noise, there are some problems such as mode mixing or over-decomposi-

tion, which affect the processing performance of these methods on engineering signals to some extent [14, 15]. Signal denoising problem has always been the hotspot in signal processing field. Up to now, different signal denoising techniques have been developed to analyze the vibration signals. Second Generation Wavelet is a spatial domain construction of biorthogonal wavelets developed by Sweldens [16, 17]. It abandons the Fourier transform as design tool for wavelets, wavelets are no longer defined as translates and dilates of one fixed function. SGW provides a great deal of flexibility, compared with classical wavelet transform, we can use any linear, non-linear, or space-varying prediction operator and update operator, and it ensures that the resulting transform is invertible [18-21].

For the above reasons, we propose a hybrid approach combining (VMD) and SGW to purify the raw signal and to extract the defect information, respectively. Firstly, the VMD is used to decompose the vibration signal of the bearing. Then, by combining the cross-correlation analysis criterion and the kurtosis criterion, an effective component is selected as the observation signal. Thirdly, SGW is used to improve the periodic impact components in the signal. Finally, the envelope spectrum is used to achieve the fault characteristic frequency.

The outline of this paper is as follows. The fundamental theories of VMD, SGW, the kurtosis criterion and the cross-correlation criterion are briefly summarized in Sec. 2. In Sec. 3, the hybrid approach is presented. The performance of the proposed method is confirmed by experimental results in Sec. 4. Finally, Sec. 5 concludes the paper.

2. Basic principle

2. 1. Principle of variational mode decomposition (VMD)

In the VMD method, the modal components are updated directly in the frequency domain, and then transformed into the time domain by inverse Fourier transform. The idea of the process is to assume that the majority of each mode is closely around a central frequency, and then transform the problem of modal bandwidth into the problem constrained optimization to solve each mode. The IMF is generally considered as amplitude modulated frequency modulated signals in the VMD algorithm and can be expressed by the following equation:

$$u_k(t) = A_k(t) \cos(\Phi_k(t)). \quad (1)$$

For the construction of the constrained variational

problem, assuming that each IMF has a $u_k(t)$ finite bandwidth, the variational problem can be expressed as seeking of K modal functions. The detailed decomposition steps are as follows:

1. For every modal component signal $u_k(t)$ unilateral frequency spectrum is achieved by the Hilbert transform:

$$\left(\delta(t) + \frac{j}{\pi t} \right) * u_k(t). \quad (2)$$

2. Added the exponential term $e^{-jw_k t}$ to regulate the estimated central frequency of analytical signals corresponding to each mode function, and shift the spectrum of each mode to the base band:

$$\left[\left(\delta(t) + \frac{j}{\pi t} \right) * u_k(t) \right] * e^{-jw_k t}. \quad (3)$$

3. Estimate the bandwidth, and the constrained variational problem is given as:

$$\left\{ \begin{array}{l} \min_{\{u_k\}, \{w_k\}} \left\{ \sum_k \left\| \partial_t \left[\left(\delta(t) + \frac{j}{\pi t} \right) * u_k(t) \right] e^{-jw_k t} \right\|_2^2 \right\}, \\ s.t. \sum_k u_k = f \end{array} \right. \quad (4)$$

where: $\{u_k\} : \{u_1, u_2, \dots, u_K\}$ and $\{w_k\} : \{w_1, w_2, \dots, w_K\}$ are mode sets and their central frequency, respectively; $\| \cdot \|_2^2$ is the square of modulus; $\delta(t)$ is an impact function; $*$ is the convolution operation.

4. The Lagrangian function L is introduced to transform that constraint into an unconstrained variational problem:

$$\begin{aligned} L(\{u_k\}, \{w_k\}, \lambda) = & \alpha \sum_k \left\| \partial_t \left[\left(\delta(t) + \frac{j}{\pi t} \right) * u_k(t) \right] e^{-jw_k t} \right\|_2^2 + \\ & + \left\| f(t) - \sum_k u_k(t) \right\|_2^2 + \left\langle \lambda(t), f(t) - \sum_k u_k(t) \right\rangle. \end{aligned} \quad (5)$$

5. The ‘‘saddle point’’ of the augmented Lagrange function L is searched through a series of iterative updates $u_k^{n+1}, w_k^{n+1}, \lambda_k^{n+1}$, and the expression of the Intrinsic Mode Functions $u_k(t)$ is:

$$\begin{aligned} u_k^{n+1} = & \arg \min_{u_k \in X} \left\{ \alpha \left\| \partial_t \left[\left(\delta(t) + \frac{j}{\pi t} \right) * u_k(t) \right] e^{-jw_k t} \right\|_2^2 + \right. \\ & \left. + \left\| f(t) - \sum_i u_i(t) + \frac{\lambda(t)}{2} \right\|_2^2 \right\}. \end{aligned} \quad (6)$$

Through Parseval / Plancherel Fourier isometry transformation, the Intrinsic Mode Functions $\{u_k\}$ and its

corresponding center frequencies $\{w_k\}$ were transformed into the frequency domain, and the solutions of quadratic optimization problems were obtained through a series of simplified transformation:

$$\hat{u}_k^{n+1}(w) = \frac{\hat{f}(w) - \sum_{i \neq k} \hat{u}_i(w) + \frac{\hat{\lambda}(w)}{2}}{1 + 2\alpha(w - w_k)^2}. \quad (7)$$

The updated algorithm of central frequency is obtained by the same method as above:

$$w_k^{n+1} = \frac{\int_0^\infty w |\hat{u}_k(w)|^2 dw}{\int_0^\infty |\hat{u}_k(w)|^2 dw}. \quad (8)$$

The implementation of the VMD method is:

- a) Initialize $\{\hat{u}_k^1\}, \{\hat{w}_k^1\}, \hat{\lambda}^1, n$;
- b) Execution cycle: $n = n + 1$;
- c) Update $\{w_k^{n+1}(w)\}$ for all $w \geq 0$:

$$\hat{u}_k^{n+1}(w) = \frac{\hat{f}(w) - \sum_{i < k} \hat{u}_i^{n+1}(w) - \sum_{i > k} \hat{u}_i^n(w) + \frac{\hat{\lambda}^n(w)}{2}}{1 + 2\alpha(w - w_k^n)^2}, \quad (9)$$

- d) Update $w_k^{n+1}(w)$:

$$w_k^{n+1} = \frac{\int_0^\infty w |\hat{u}_k^{n+1}(w)|^2 dw}{\int_0^\infty |\hat{u}_k^{n+1}(w)|^2 dw}. \quad (10)$$

- e) Dual ascent for $w \geq 0$:

$$\hat{\lambda}^{n+1}(w) \leftarrow \hat{\lambda}^n(w) + \tau \left(\hat{f}(w) - \sum_k u \right). \quad (11)$$

- f) Continue the iteration until the condition of convergence is satisfied:

$$\sum_k \left\| \hat{u}_k^{n+1} - \hat{u}_k^n \right\|_2^2 / \left\| \hat{u}_k^n \right\|_2^2 < \varepsilon. \quad (12)$$

Hilbert transformation can be performed for all mode function to obtain meaningful instantaneous frequency, instantaneous amplitude and the Hilbert spectrum.

2.2. Denoising algorithm based on Second Generation Wavelet (SGW)

Second-generation wavelet (SGW) is a new wavelet theory that emerged in recent years. Compared with the traditional wavelet, the construction of SGW avoids Fourier

transform. In addition, it has fast computational speed. Because of the advantages of SGW, it has been widely applied in vibration signal processing field. For example, Li et al. [14] combined lifting wavelet with morphological wavelet to construct an adaptive morphological gradient lifting wavelet, which is used for bearing and gear vibration signal denoising and feature extraction.

The second generation wavelet method is proposed by Sweldens W. in 1995 [16]. It is a fast and efficient wavelet transforming technique. Different from the traditional WT, the second generation wavelet (SGW) is a flexible wavelet construction method which is independent of the Fourier transform. In addition, it has fast computational speed, it has been widely applied in vibration signal processing field. SGW inherited its excellent characteristics of time-frequency location. Furthermore, SGW has higher calculation efficiency and more clear principle and needs lower space [17]. SGW transform includes decomposition and reconstruction processes. The decomposition stage of SGW can be summarized as follows.

The reconstruction stage of SGW is a reverse procedure of the decomposition stage.

1. Split: the signal $X = \{x[n], n \in Z\}$ is divided into two subsets: the odd sample set $X_o = \{x_o[n], n \in Z\}$ and the even sample set $X_e = \{x_e[n], n \in Z\}$:

$$\begin{aligned} x_o[n] &= x[2n+1] \\ x_e[n] &= x[2n] \end{aligned} \quad (13)$$

2. Predict: the prediction operator is used to predict the odd sample set X_o on the even sample set X_e . Then, the prediction error between $x_o[n]$ and $P(X_e)$ gives the detail coefficients $d[n]$:

$$d[n] = x_o[n] - P(X_e). \quad (14)$$

3. Update: use the update operator U to update the detail coefficients $D = \{d[n], n \in Z\}$ and add the result $U(D)$ to $x_e[n]$; the approximation coefficients $c[n]$ can be obtained:

$$c[n] = x_e[n] + U(D). \quad (15)$$

After the above three steps, the detail coefficients $D = \{d[n], n \in Z\}$ and the approximation coefficients $C = \{c[n], n \in Z\}$ are obtained. Multilayer decomposition of SGW can be carried out through the iteration of these three steps. Here, the prediction operator $P = [p(1), p(2), \dots, p(M)]$ and update operator $U = [u(1), u(2), \dots, u(N)]$ is vector with length of M and N , respectively. They can be designed by interpolating subdivision method. The obtained SGW is denoted as (M, N) SGW and the reconstruction stage of SGW is a reverse procedure of the decomposition stage.

2.3. Cross-Correlation coefficient and Kurtosis

The correlation coefficient can be used as an index to calculate the degree of correlation between two signals. The larger the correlation coefficient value, the higher the correlation with the original signal. By using this criterion, the degree of correlation between each component signal obtained from the decomposition and the original signal can be known. The computation procedure of the correlation number is as follows:

$$r = \frac{\sum_{i=0}^n (x_i - \bar{x})(y_i - \bar{y})}{\sqrt{\sum_{i=0}^n (x_i - \bar{x})^2 (y_i - \bar{y})^2}}, \quad (16)$$

where: x_i and \bar{x} are specific values and average values of the signal x . At the same time, y_i and \bar{y} are specific values and average values of the signal y , respectively. Kurtosis can be used to determine the peak degree of signal waveform, and it is more sensitive to the impact components in the signal. The higher the proportion of impact components is, the higher the kurtosis value will be. For bearings, the kurtosis value is close to the normal distribution under normal operation, and it will increase significantly when faults occur. The computation method is as follows:

$$K_i = \frac{1}{n} \sum_{i=1}^n \left(\frac{x_i - \bar{x}}{\sigma} \right)^4, \quad (17)$$

where: x_i and \bar{x} are specific values and average values of the signal x , σ is the standard deviation of the signal, and n is the number of samples [22-24].

3. The steps of the proposed method

Rolling element bearing is extensively used in rotating machinery, and it is one of the most essential and vulnerable parts. If the fault features information can be extracted successfully at the early stage of the bearing failure, and correctly identify the bearing running condition, timely repair or replace damaged bearing, can effectively shun catastrophic failures, which is of great significance to improve product performance and decrease economic losses.

However, the vibration signals collected by the sensors are accompanied by a large number of interference signals, which makes the signals have weak and unstable characteristics. Consequently, how to efficiently extract the defect features, analyze the fault feature frequency, and judge the fault type has always been a concern of people, and it is also a hotspot research problem for non-stationary and non-Gaussian vibration signals.

To find a suitable and effective tool for bearing fault diagnosis a few of steps are developed in this paper:

Step 1. VMD algorithm decomposes the signal into a combination of multiple modal components IMFs and can suppress the modal aliasing phenomenon.

Step 2. Obtain the kurtosis value and correlation coefficient, and select the optimum IMFs components.

Step 3. The (SGW) algorithm can remove out most of the noise in the optimum IMFs and reveal the impact components of the fault.

Step 4. The selected IMFs are reconstructed and analyzed by envelope spectrum to extract the fault characteristic frequency.

4. Experimental apparatus and data collection

In order to confirm the success of the proposed scheme for noise reduction and defect feature enhancement of rolling bearing fault signals, the bearing data of Case Western Reserve University in the United States are selected. Single point faults produced by electro-discharge machining were caused in the test bearings. The test uses the 6205-2RS-JEM-SKF deep groove ball bearing. These signals were taken from an accelerometer mounted on the bearing housing at the drive end of the induction motor which is connected to a torque transducer, coupled to a dynamometer. The data were saved as different files in MATLAB format. Detailed information is shown on the CWRU bearing data center website [25]. In this paper, the sampling frequency is 12 kHz and the motor speed is 1797 rpm. The basic geometric parameters are shown in Table 1. Usually, the bearing fault frequencies are calculated in the time domain based on the number of impulses generated for one complete revolution of the shaft. However, the defect frequencies can be calculated mathematically from the pitch diameter, ball diameter, number of balls, contact angle and

revolution rate of the shaft. From the physical dimensions and the operating speed, the different fault frequencies can be calculated as described in the equations below.

Outer race defect frequency:

$$BPFR = \frac{D}{2d} \left(1 - \left(\frac{d}{D} \right)^2 \cos^2 \alpha \right) \times f_r. \quad (18)$$

Inner race defect frequency:

$$BPFO = \frac{Z}{2} \left(1 - \frac{d}{D} \cos \alpha \right) \times f_r. \quad (19)$$

Rolling element frequency:

$$BPFI = \frac{Z}{2} \left(1 + \frac{d}{D} \cos \alpha \right) \times f_r, \quad (20)$$

where: Z is the number of rolling elements; d is the rolling element diameter; D is the bearing pitch diameter; α is the contact angle; f_r is the shaft rotation frequency, Hz. Based on the bearing parameters shown in Table. 1 and equations (18 – 20), the fault characteristic frequency of the rolling bearing, $BPFO = 107.36$ Hz; $BPFI = 162.19$ Hz; and $BPFR = 141.1693$ Hz, respectively.

Table 1

The basic geometric parameters of SKF 6205

Rolling element number, Z	Inner diameter, inches	Outer diameter, inches	Rolling element diameter d , inches	Contact angle α	Pitch circle diameter D , inches	Speed, rpm
9	0.984	2.047	0.312	00	1.532	1797

5. Results and discussion

5.1. Bearing inner race fault detection

When a bearing fault of inner ring happens, its location, where the balls pass through, varies because of the rotating of inner ring with the shaft, so an impulse feature will be repeated by the frequent of rotating. By mathematical calculations, the ball passing frequency inner race ($BPFI = 162.19$ Hz). The time domain and the frequency domain of the bearing inner ring fault signal are shown in Fig. 1. Due to the interference of the background noise, characteristic frequency related to bearing fault is masked and it is difficult to separate the periodic pulse features, hence it is impossible to extract the fault characteristic information directly from the time domain and the frequency domain.

To testify the effectiveness of the proposed method, the signal is decomposed by the VMD. As revealed in Fig. 2, VMD method can decompose a bearing non-stationary vibration signals with inner raceway fault into a sum a plurality of stationary component IMFs.

The kurtosis and the cross-correlation coefficients value of each component are calculated; in this study the signal components with kurtosis value bigger than 3 and correlation coefficient bigger than 0.3 are selected. It can be seen from Table 2 that the signal components of IMF4 and IMF5 are carefully chosen in our analysis. Then they are de-

noised with the SGW and superimposed to reconstruct a new signal.

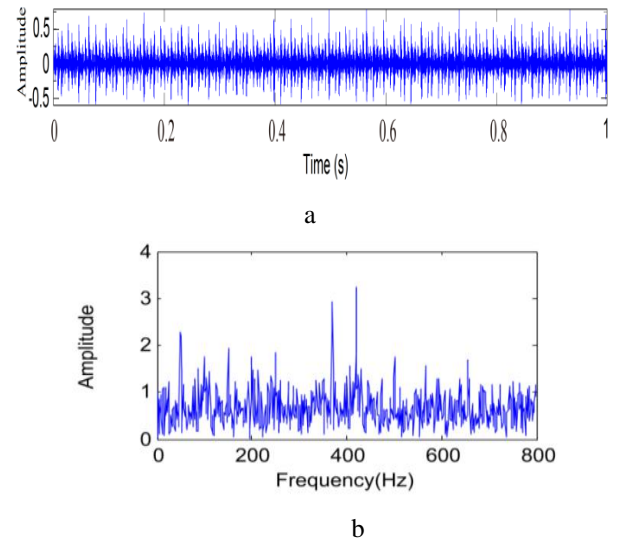


Fig. 1 Vibration signal of bearing with an inner race fault: a) Time - domain; b) Frequency - domain

After the noise reduction by SGW, it can be seen from Fig. 3, a that the majority of the noise is successfully filtered and the waveform of the reconstructed signal is very analogous to the original inner ring fault signal, as well the

periodic fault shock components has really observed in the reconstructed signal. By applying the envelope spectrum of the reconstructed signal, it can be observed from Fig. 3, b that the characteristic frequency of the fault is obvious and the frequencies are very close to the theoretical calculated values; this means that the choice of key parameters is significantly vital in fault diagnosis. Consequently, the results demonstrate that the fault of bearing inner ring can be accurately diagnosed by the proposed technique.

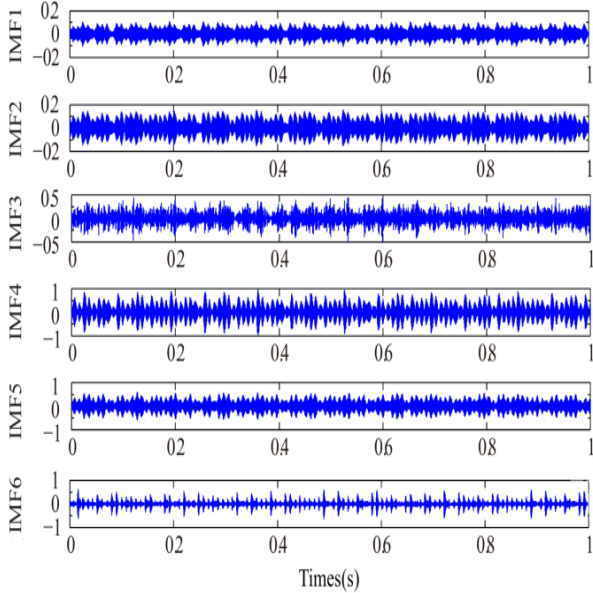


Fig. 2 the decomposed IMFs of the inner raceway fault signal using VMD

Table 2

The kurtosis and the cross-correlation coefficients

IMF	1	2	3	4	5	6
kurtosis	1.305	2.543	3.576	3.768	4.564	2.904
the cross-correlation coefficients	0.035	0.178	0.265	0.386	0.453	0.268

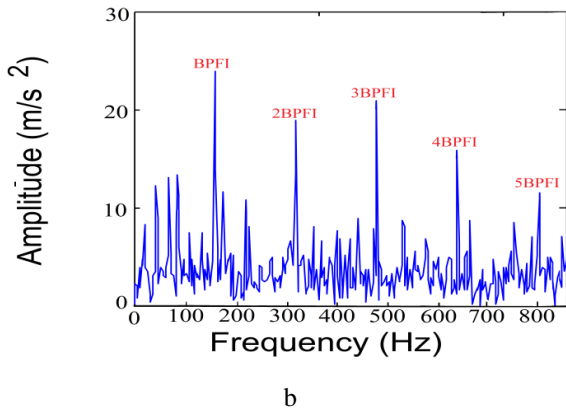
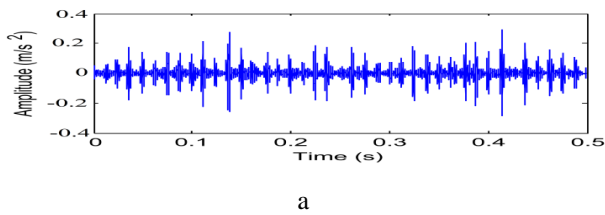


Fig. 3 a) The reconstructed signals; b) Its envelope spectrum

5.2. Bearing outer race fault detection

When a bearing fault of outer ring happens, its position is unvaried. An impulse feature will be repeated by the fault characteristic frequency of outer ring.

According to theoretical computations, the ball passing frequency outer race ($BPFO = 107.36$ Hz). The time domain and the frequency domain of the bearing outer ring fault signal are shown in Fig. 4. Due to the existing of strong noise; it is difficult to extract the fault feature frequency. As we know, VMD can decompose a complex multicomponent signal into a series of sub-signals, which are mostly compact around a center pulsation, with a limited frequency bandwidth.

To prove the success of our approach of bearing fault diagnosis, VMD method is applied to the signal, and the decomposed results are shown in Fig. 5.

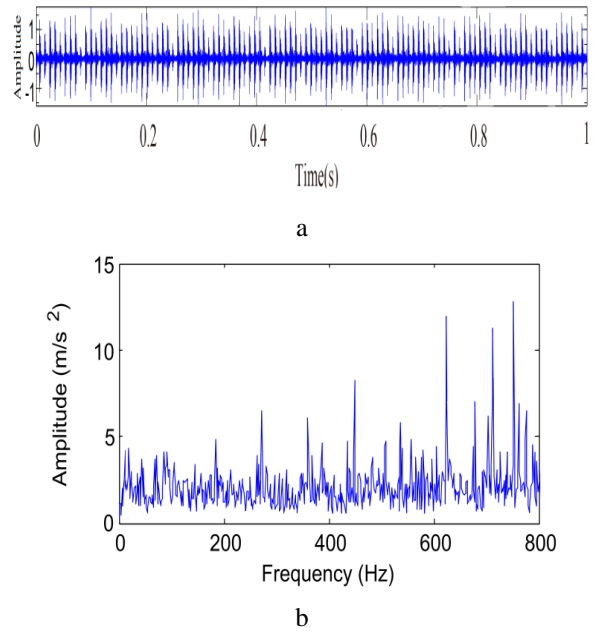


Fig. 4 Vibration signal of bearing with an outer race fault: a) Time-domain; b) Frequency-domain

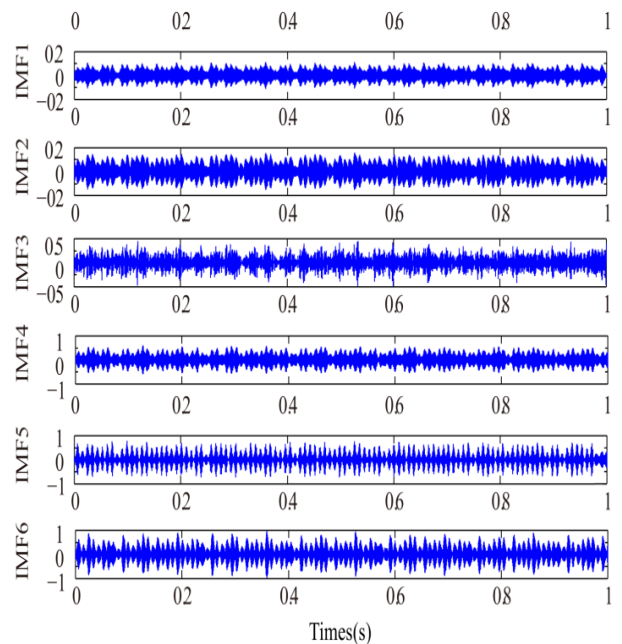


Fig. 5 The decomposed IMFs of the outer raceway fault signal using VMD

Via calculating the cross-correlation coefficients and kurtosis value of each signal component, the results are shown in Table. 3, it can be seen that three IMF components (i.e. IMF3, IMF4, and IMF5) have better fault information than other IMFs, so the three IMFs are denoised by SGW and used to reconstruct the vibration signal.

Table 3

The kurtosis and the cross-correlation coefficients

IMF	1	2	3	4	5	6
kurtosis	1.223	1.786	3.045	3.276	4.353	2.643
the cross-correlation coefficients	0.017	0.132	0.303	0.365	0.398	0.232

The reconstructed signal and its envelope spectrum are correspondingly showed in Fig. 6. It can be evidently seen after noise reduction by SGW that the periodic fault impact component of the outer ring fault signal has been extracted and the useful fault signatures can be clearly revealed. As can be seen in the achieved envelope spectrum of the filtered signal that the fault frequency (106, 41 Hz) and its first three harmonics (213.2 Hz), (320.1 Hz), (426.1 Hz) can be observed in Fig. 6, b, this means that the proposed method detect the outer race bearing damage effectively.

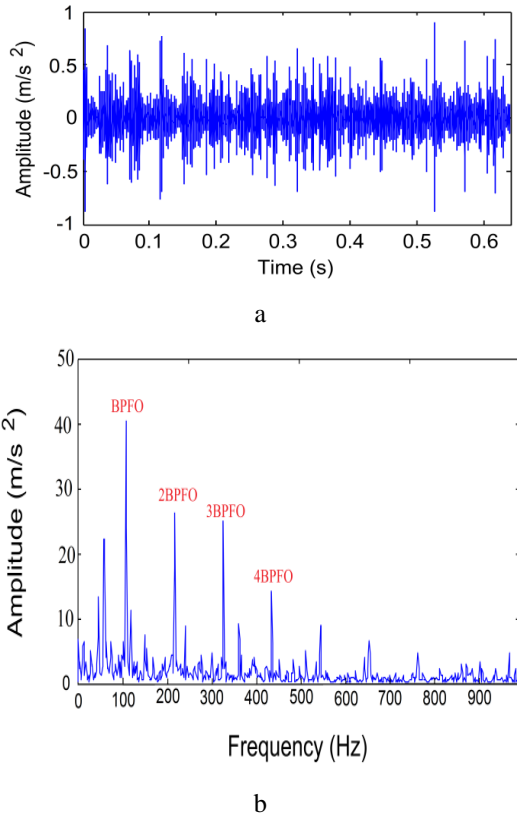


Fig. 6 a) The reconstructed signals; b) Its envelope spectrum

5.3. Rolling element fault detection

The rolling element fault is analysed more difficultly, because the fault point is continuously in motion status following the rolling elements rotating. However, weak signatures in the time domain are often contaminated because the intervention of strong ambient noises, the time domain and the frequency domain are shown in Fig. 7

Then, the VMD method is used to decompose the signal of the rolling element and 6 IMFs components are obtained, the decomposition results are shown in Fig. 8.

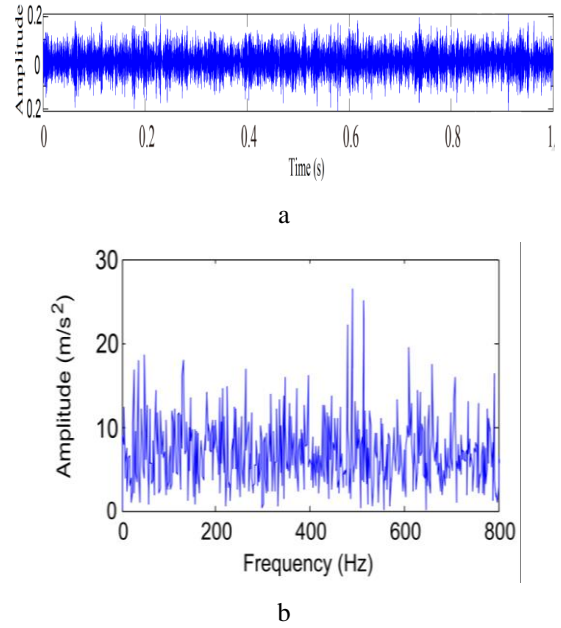


Fig. 7 Vibration signal of bearing with a rolling element fault: a) Time-domain; b) Frequency-domain

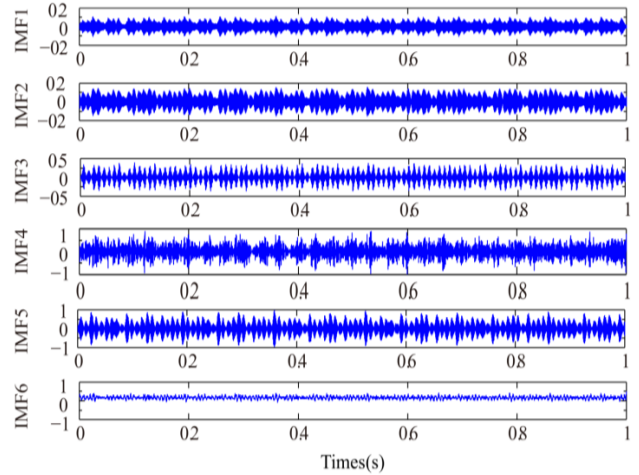


Fig. 8 the decomposed IMFs of the rolling element fault signal using VMD

The kurtosis and cross-correlation coefficients each component is shown in Table 4. One can observe explicitly that only the IMF4 component meets the set threshold conditions. Therefore, it is selected to de-noise with the SGW and reconstructed.

Table 4

The kurtosis and the cross-correlation coefficients

IMF	1	2	3	4	5	6
kurtosis	1.112	1.966	2.645	3.836	2.773	2.163
the cross-correlation coefficients	0.107	0.235	0.283	0.385	0.268	0.239

It can be clearly seen from the reconstructed signal that the impulsive features and periodic fault shock component of the rolling element fault signal is successfully extracted as well noises are successfully removed. In addition,

we can observe from the envelope spectrum in Fig. 9, b that the rolling element defect frequency 140.6 Hz, and its frequency doubling 281.3 Hz are rather clear and the peaks at defect frequency are very obvious and prominent. The results show that the proposed scheme is still capable to diagnose the rolling element defect.

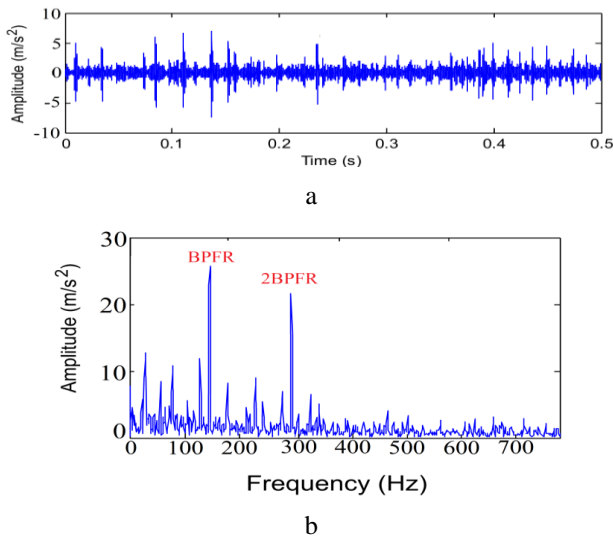


Fig. 9 a) The reconstructed signals; b) Its envelope spectrum

6. Conclusions

An unexpected malfunction of a rolling bearing may cause the sudden breakdown of rotating machinery. However, the measured vibration signals are complex and non-stationary in nature, and meanwhile impulsive signatures of rolling bearing are generally engrossed in noise.

After the analysis of bearing fault signals, the conclusions reached are as follows:

1. A set of Intrinsic Mode Function components (IMFs) can be got by VMD and the modal aliasing can be suppressed.
2. Via calculating of cross-correlation analysis and kurtosis, the optimum signal components are carefully chosen and used to reconstruct the vibration signal.
3. By using (SGW) the most of the noise can be removed and the periodic impact component can be successfully improved.
4. The envelope spectrum shows that the proposed technique can perfectly extract the characteristic frequency of faults in a strong noise background environment.

References

1. **Rubini, R.; Meneghetti, U.** 2001. Application of the envelope and wavelet transform analyses for the diagnosis of incipient faults in ball bearings, *Mechanical Systems & Signal Processing* 15(2): 287-302. <https://doi.org/10.1006/mssp.2000.1330>.
2. **Lv, Y.; Yuan, R.; Song, G.** 2016. Multivariate empirical mode decomposition and its application to fault diagnosis of rolling bearing, *Mechanical Systems & Signal Processing* 81: 219-234. <https://doi.org/10.1016/j.ymssp.2016.03.010>.
3. **Wei Li, Zhencai Zhu, Fan Jiang,** et al. 2015. Fault diagnosis of rotating machinery with a novel statistical feature extraction and evaluation method, *Mechanical Systems and Signal Processing* 50-51: 414-426. <http://dx.doi.org/10.1016/j.ymssp.2014.05.034>.
4. **Zhu, L.; He, F.; Tong Y.; Li, D.** 2015. Fault detection and diagnosis of belt weighed using improved DBSCAN and Bayesian regularized neural network. <http://dx.doi.10.5755/j01.mech.21.1.8560>.
5. **Dyballa, J.; Zimroz, R.** 2013. Rolling bearing diagnosing method based on empirical mode decomposition of machine vibration signal *Appl, Acoust* 77: 195-203. <https://doi.org/10.1016/j.apacoust.2013.09.001>.
6. **Amarnath, M.; Krishna, I. P.** 2012. Empirical mode decomposition of acoustic signals for diagnosis of faults in gears and rolling element bearings, *IET. Sci. Mea. Technol* 6: 279-287. <https:// DOI: 10.1049/iet-smt.2011.0082>.
7. **Smith, J. S.** 2005. The local mean decomposition and its application to EEG perception date, *JR Soc interface* 2(5): 443-454. <https://doi.org/10.1098/rsif.2005.0058>.
8. **Gao, Q.; Duan, C.; Fan, H.** et al. 2008. Rotating machine fault diagnosis using empirical mode decomposition, *Mechanical Systems and Signal Processing* 22(5): 1072-1081. <https://doi.org/10.1016/j.ymssp.2007.10.003>.
9. **Wang, Y.; He, Z.; Zi, Y.** 2010. A comparative study on the local mean decomposition and empirical mode decomposition and their applications to rotating machinery health diagnosis, *J. Vib. Acoust.* 132 (2). <https://doi.org/10.1115/1.4000770>.
10. **Dragomiretskiy, K.; Zosso, D.** 2014. Variational mode decomposition, *IEEE. T. Signal Process* 62: 531-544. <https://doi: 10.1109/TSP.2013.2288675>.
11. **Zhang, S.; Wang, Y.; He, S.; Jiang, Z.** 2016. Bearing fault diagnosis based on variational mode decomposition and total variation denoising, *Meas. Sci. Technol.* 27(7). <https://doi: 10.1088/0957-0233/27/7/075101>.
12. **Wang, Y.; Markert, R.; Xiang, J.; Zheng, W.** 2015. Research on variational mode decomposition and its application in detecting rub-impact fault of the rotor system, *Mech. Syst. Signal. Process* 60: 243-251. <https://doi: 10.1016/j.ymssp.2015.02.020>.
13. **Lv, Z.; Tang, B.; Zhou, Y.; Zhou, C.** 2016. A novel method for mechanical fault diagnosis based on variational mode decomposition and multikernel support vector machine, *Shock Vib.* <https://doi: 10.1155/2016/3196465>.
14. **Li, Z.; Jiang, Y.; Guo, Q.; Hu, C.; Peng, Z.** 2016. Multi-dimensional variational mode decomposition for bearing-crack detection in wind turbines with large driving-speed variations, *Renew. Energ* 116: 55-73. <https://doi.org/10.1016/j.renene.2016.12.013>.
15. **Li, B.; Zhang, P.; Mi, S.; Hu, R.; Liu, D.** 2012. An adaptive morphological gradient lifting wavelet for detecting bearing defects, *Mechanical Systems and Signal Processing* 29: 415-427. <https://doi:10.1016/j.ymssp.2011.12.016>.
16. **Fan, X.; Liang, M.; Yeap, T. H.; Kind, B.** 2007. A joint wavelet lifting and independent component analysis approach to fault detection of rolling element bearings, *Smart Materials and Structures* 16 (5): 1973-1987. <https://doi:10.1088/0964-1726/16/5/056#>.
17. **Cao, S.; Chen, X.** 2005. The second-generation wavelet transform and its application in denoising of seismic data, *Appl. Geophys* 2: 70-74.

- <https://doi.org/10.1007/s11770-005-0034-4>.
18. **Na Lu.; Guangtao Zhang.; Yuanchu Cheng.; Diyi Chen.** 2016. Signal Denoising Method Based on Adaptive Redundant Second-Generation Wavelet for Rotating Machinery Fault Diagnosis, *Mathematical Problems in Engineering*.
<http://dx.doi.org/10.1155/2016/2727684>.
 19. **Dong, W.; Peter, W.; Kwok, T.** 2013. An enhanced Kurtogram method for fault diagnosis of rolling element bearings, *Mechanical Systems and Signal Processing* 35: 176-199.
<http://doi:10.1016/j.ymssp.2012.10.003>.
 20. **Qin, S. R.; Zhong, Y. M.** 2006. A new envelope algorithm of Hilbert-Huang Transform, *Mechanical Systems and Signal Processing*, 20(8): 1941-1952.
<https://doi.org/10.1016/j.ymssp.2005.07.002>.
 21. **He, W.; Jiang, Z.N.; Qin, Q.** 2010. A joint adaptive wavelet filter and morphological signal processing method for weak mechanical impulse extraction, *J. Mech. Sci. Technol.* 24(8): 1709-1716.
<http://dx.doi.org/10.1007/s12206-010-0511-4>.
 22. **Wang, Y.; Xiang, J.; Richard, M.** 2016. Spectral kurtosis for fault detection, diagnosis and prognostics of rotating machines, A review with applications, *Mechanical Systems and Signal Processing* 66: 679-698.
<http://doi:10.1016/j.ymssp.2015.04.039>.
 23. **Antoni, J.; Randall, R. B.** 2006. The spectral kurtosis: application to the vibratory surveillance and diagnostics of rotating machines, *Mechanical System and Signal Processing* 20: 308-331.
<https://doi.org/10.1016/j.ymssp.2004.09.002>.
 24. **Lei, Y. G.; Lin, J.; He, Z. J.** 2011. Application of an improved kurtogram method for fault diagnosis of rolling element bearings, *Mech. Syst. Signal Process* 25(1): 1738-1749.
<http://dx.doi.org/10.1016/j.ymssp.2010.12.011>.
 25. **Dr. Kenneth A. Loparo.** Bearing data center [EB/OL], Case Western Reserve University.
<http://csegroups.case.edu/bearingdatacenter/home>.

T. Bensana, S. Mekhilef, M. Mihoub, M. Fnides

A NOVEL METHOD FOR BEARING FAULT DIAGNOSIS BASED ON VMD AND SGW

S u m m a r y

The bearing vibration signal with strong non-stationary properties is generally composed of multiple components making it complicated to extract the characteristic fault features of vibration signals of rolling bearings under the background of strong noise, how to solve this problem effectively is the focus of our research. Therefore, a new scheme based on Variational Mode Decomposition (VMD) and second-generation wavelet (SGW) is proposed in this paper. Firstly, VMD can decompose accurately and adaptively a complex multi-component signal into a set of IMF component with narrow band properties. Secondly, on the basis of kurtosis and cross-correlation analysis, the optimum signal components obtained by the VMD are selected to filter and to reconstruct the analysis signal. Then, (SGW) approach is used to eliminate the strong noise background and enhance the periodic impact in the optimum IMF components. Lastly, the accurate characteristic defect frequency can be obtained by using envelope spectrum of the reconstructing signal. The success of the proposed approach is verified by analysis the vibration signals of bearings with an outer race, an inner race and a rolling element faults, respectively. The results indicate that the scheme is feasible and useful for extracting the bearings fault features.

Keywords: Fault diagnosis, rolling bearing, variational mode decomposition, second generation wavelet.

Received February 22, 2021

Accepted April 08, 2022



This article is an Open Access article distributed under the terms and conditions of the Creative Commons Attribution 4.0 (CC BY 4.0) License (<http://creativecommons.org/licenses/by/4.0/>).